Solar and Stellar Magnetic Fields: Origins and Manifestations
Proceedings IAU Symposium No. 354, 2019
A. Kosovichev, K. Strassmeier & M. Jardine, ed.
doi:10.1017/S1743921319010032

The 3D structure of the penumbra at high resolution from the bottom of the photosphere to the middle chromosphere

Mariarita Murabito[1], Ilaria Ermolli[1], Fabrizio Giorgi[1], Marco Stangalini[1], Salvo L. Guglielmino[2], Shahin Jafarzadeh[3,4], Hector Socas-Navarro[5,6], Paolo Romano[7] and Francesca Zuccarello[2]

[1]INAF–Osservatorio Astronomico di Roma,
Via Frascati 33, I-00078, Monte Porzio Catone, Italy
email: mariarita.murabito@inaf.it

[2]Dipartimento di Fisica e Astonomia–Sezione Astrofisica
Università degli studi di Catania, Via S. Sofia 78, I-95123 Catania, Italy

[3]Rosseland Centre for Solar Physics, University of Oslo,
P.O. BOX 1029 Blindern, NO-0315 Oslo, Norway

[4]Institute of Theoretical Astrophysics, University of Oslo,
P.O. BOX 1029 Blindern, NO-0315 Oslo, Norway

[5]Instituto de Astrofisica de Canarias,
C/Via Lactea s/n, E-38205 La Laguna, Tenerife, Spain

[6]Departimento de Astrofisica, Universidad de La Laguna,
E-38205 La Laguna, Tenerife, Spain

[7]INAF–Osservatorio Astrofisico di Catania,
Via S. Sofia 78,I-95123, Catania, Italy

Abstract. Sunspots are the most prominent feature of the solar magnetism in the photosphere. Although they have been widely investigated in the past, their structure remains poorly understood. Indeed, due to limitations in observations and the complexity of the magnetic field estimation at chromospheric heights, the magnetic field structure of sunspot above the photosphere is still uncertain. Improving the present knowledge of sunspot is important in solar and stellar physics, since spot generation is seen not only on the Sun, but also on other solar-type stars. In this regard, we studied a large, isolated sunspot with spectro-polarimeteric measurements that were acquired at the Fe I 6173 nm and Ca II 8542 nm lines by the spectropolarimeter IBIS/DST under excellent seeing conditions lasting more than three hours. Using the Non-LTE inversion code NICOLE, we inverted both line measurements simultaneously, to retrieve the three-dimensional magnetic and thermal structure of the penumbral region from the bottom of the photosphere to the middle chromosphere. Our analysis of data acquired at spectral ranges unexplored in previous studies shows clear spine and intra-spine structure of the penumbral magnetic field at chromopheric heights. Our investigation of the magnetic field gradient in the penumbra along the vertical and azimuthal directions confirms results reported in the literature from analysis of data taken at the spectral region of the He I 1083 nm triplet.

Keywords. Sun: magnetic fields, Sun: chromosphere, Sun: photosphere

1. Introduction

Space- and ground-based observations have been used to study the sunspot penumbra, from its formation (Murabito *et al.* 2016, 2017, 2018) to the three dimensional (3D) magnetic structure (Joshi *et al.* 2016, 2017). Balthasar 2018 reported about the unsolved problem of the estimation of the magnetic field gradient in sunspots and how this gradient changes due to the different techinque employed. All previous studies were on photospheric observations taken through several lines, but only one chromospheric data acquired at the He I triplet at 1083.0 nm. Recently, a different chromospheric diagnostic, the Ca II 854.2 nm line, was used by Joshi & de la Cruz Rodríguez 2018 to study the variation of atmospheric parameters associated with umbral flashes, reporting a decrease of the magnetic field of -0.5 G km^{-1} when moving from the photosphere to the chromosphere. In this contribution, we summarize the results obtained from our study of the vertical gradient of the magnetic field in a sunspot penumbra, based on photospheric Fe I 617.3 nm and chromospheric Ca II 854.2 nm lines.

2. Observations

We used data acquired on 2016 May 20 at the Dunn Solar Telescope of the National Solar Observatory. The data consists of spectropolarimetric observations of a large sunspot located near the disk center in photosphere and chromosphere taken at the Fe I 617.3 nm and Ca II 854.2 nm lines. These data were obtained from the Interferometric BIdimensional Spectrometer (IBIS, Cavallini 2006) at 21 spectral points for both lines, with a spectral sampling of 20 mÅ and 60 mÅ for the Fe I and Ca II lines, respectively. The data were inverted with the Non-LTE inversion COde (NICOLE Socas-Navarro *et al.* 2015) to infer the magnetic field at the atmospheric heigths sampled by the data. For further details about the observations, data reduction and data inversion, see Stangalini *et al.* 2018 and Murabito *et al.* 2019.

Based on the results from the response functions (RFs) computation, we focused our analysis to the plasma conditions at three atmospheric heigths in the photosphere ($\log \tau \approx -0.5$, -1.0, and -1.5) and one in the chromosphere ($\log\tau \approx -4.6$).

3. Results

Fig. 1 shows circular and linear polarization maps derived from the measurements taken at the Fe I and Ca II lines. The photospheric spine/intraspine structure of the penumbra is clearly displayed in panels a and b, while the same is attenuated in chromosphere as obtained from the circular and linear polarization signals estimated from the Ca II data. We derived the vertical gradient of the magnetic field strength following the formula:

$$\left(\frac{\Delta B}{\Delta log\tau}\right)_{a,b} = \frac{(\Delta B)_{a,b}}{(\Delta log\tau)_{a,b}} = \frac{B(b) - B(a)}{b - a} \tag{3.1}$$

used by Joshi *et al.* 2017, where a and b denote the lower and upper $\log \tau$, respectively. Fig. 2 (top panels) shows the maps of $(\Delta B/\Delta log\tau)$ for the subfov A marked in Fig. 1. In particular, the panel a displays the photospheric vertical gradient of the magnetic field by considering as [a,b] = [$\log \tau = -0.5$, $\log \tau = -1.5$], while the rigth panel shows the gradient between the photosphere and the chromosphere when [a,b] = [$\log \tau = -1$, $\log \tau = -4.6$]. The photospheric vertical gradient exhibits a ring-like structure, where the gradient has negative values, meaning that the magnetic field decreases with optical depth. The outer penumbra, instead, is charactherized by postive values. The radial dependence of the vertical gradient was calculated considering the average field values along 80 isocontours in the Fe I line continuum. This radial dependence is shown in Fig. 2 panels c and d. In particular, we can note that in the inner penumbra at $r/R_{spot} = 0.5$ the gradient has values of about -100 G/$\log \tau$. Moving onward to $r/R_{spot} = 0.6$, it sligthly increase reaching average values of about 300 G/ $\log \tau$.

On the other hand, both the map and the plot of the gradient between photosphere and chromosphere (panel b and d) show that in the inner penumbra, at $r/R_{spot} = 0.5$, the values are about 200 G/$\log \tau$. Moving away from the inner to the outer penumbra,

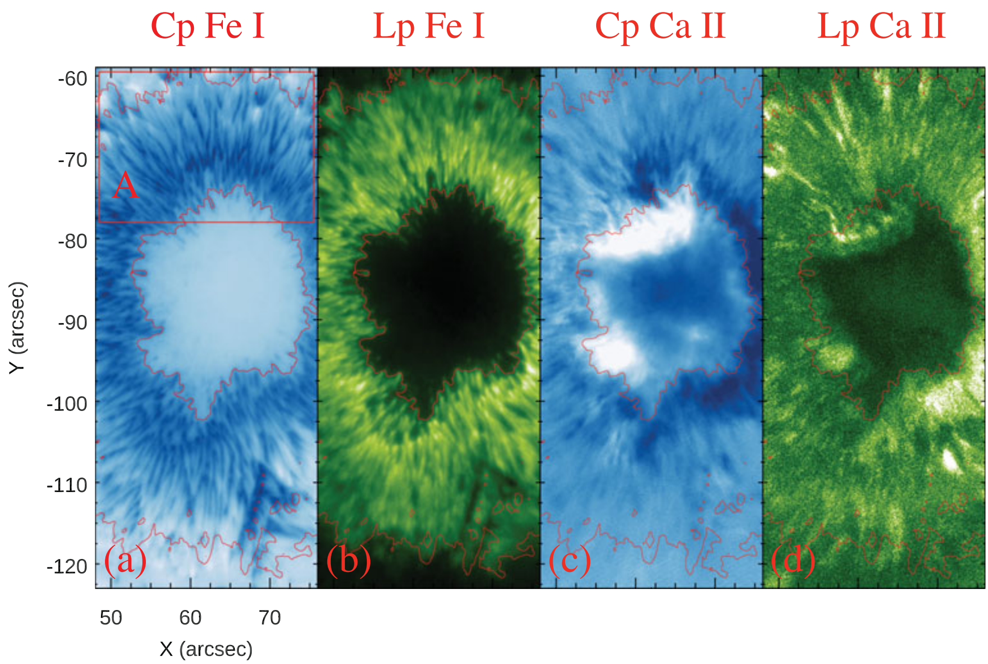

Figure 1. Circular and linear polarization maps derived from the IBIS Fe I (panels a and b) and Ca II (panels c and d) data. The red contours represent the umbra-penumbra (UP) boundary and the outer penumbra contour. The red box labelled with A indicates the subfov used for the analysis shown in Fig. 2.

the gradient slowly decreases, with an average value of 170 G/log τ up to $r/R_{spot} = 0.6$, then it has a constant value of 100 G/log τ.

4. Implications

We presented the analysis of photospheric and chromospheric data taken at different spectral range and inverted with different methods than those reported in the literature. We estimated the vertical gradient of the magnetic field strength in the photosphere and chromosphere. The ring-like structure visible in the maps of the photospheric vertical gradient derived from our study is similar to the one reported by Joshi *et al.* 2017 even if our average gradient is higher. We estimated the gradient beetween the photosphere and the chromosphere at the atmospheric heigths more sensitive to field pertubations in our data. The field gradient in the chromosphere assumes an average value of 100 G/logτ, corresponding to $\approx 0.3\ G\ km^{-1}$. This value is within the range of values reported by Joshi *et al.* 2017 from analysis of data taken at the He I 1083.0 nm.

We conclude that in order to produce a complete 3D magnetic picture of the penumbra at higher atmospheric heigths an analysis of multiple spectral diagnostics of the photosphere and chromosphere is needed.

Acknowledgments

The research leading to these results has received funding from the European Research Council under the European Union's Horizon 2020 Framework Programme for Research and Innovation, grant agreements H2020 PRE-EST (no. 739500) and H2020 SOLARNET

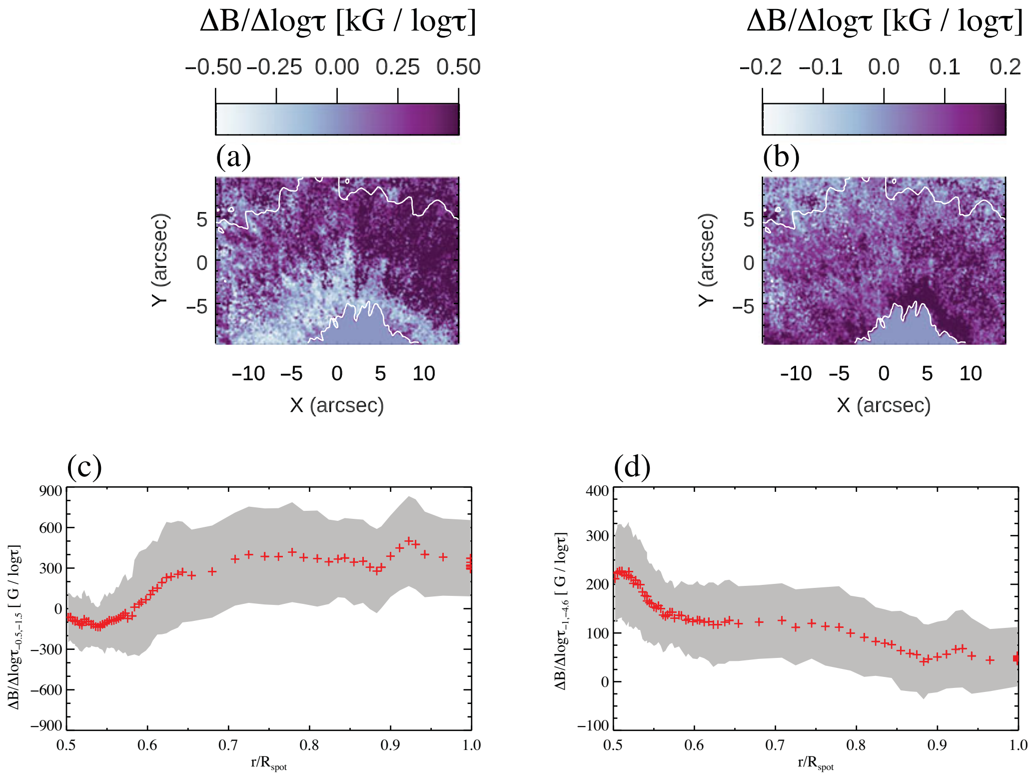

Figure 2. Top panels: Maps of the vertical gradient of the magnetic field strength considering two atmospheric heights in the photosphere (left panel) and two heights representative of the photosphere and chromosphere (rigth panel). Bottom panels: Variation of the vertical gradient as a function of r/R$_{spot}$ for the subarray A displayed in the top panels.

(no. 824135). This work was also supported by INAF Istituto Nazionale di Astrofisica (PRIN-INAF-2014).

S.J. acknowledges support from the European Research Council under the European Union's Horizon 2020 research and innovation programme (grant agreement no. 682462) and from the Research Council of Norway through its Centres of Excellence scheme (project no. 262622).

References

Balthasar H. 2018, *Solar Physics*, 293, 120
Stangalini M., Jafarzadeh S., Ermolli I., *et al.* 2018, *ApJ*, 869, 110
Murabito M., Romano P., Guglielmino S. L., *et al.* 2016, *ApJ*, 825, 75
Murabito M., Zuccarello F., Guglielmino S. L., *et al.* 2018, *ApJ*, 885, 58
Murabito M., Romano P., Guglielmino S. L., *et al.* 2017, *ApJ*, 834, 76
Joshi J., Lagg J., Solanki S. K., *et al.* 2016, *A&A*, 596, A8
Joshi J., Lagg J., Hirzberger J., *et al.* 2017, *A&A*, 604, A98
Joshi J., Lagg J., Hirzberger J., *et al.* 2017, *A&A*, 599, A35
Cavallini F. 2006, *Solar Physics*, 236, 415
Socas-Navarro H., de la Cruz Cruz Rodríguez J., Asensio Ramos A., *et al.* 2015, *A&A*, 577, A7
Murabito M., Ermolli I., Giorgi F., *et al.* 2019, *Apj*, 873, 126
Tiwari S., K., van Noort, M., Lagg, A., *et al.* 2013, *A&A*, 557, A25
Joshi, J. & de la Cruz Rodríguez, J. 2018, *A&A*, 619, A63